AIIM

Association for Information and Image Management

1100 Wayne Avenue, Suite 1100
Silver Spring, Maryland 20910

301/587-8202

Centimeter

Inches

1 of 1

Conf-940668--3

Review Copy

Comparison of the KAMELEON Fire Model to Large-Scale Open Pool Fire Data

SAND 93-2416C

V. F. Nicolette[1] and L. A. Gritzo
Thermal & Fluid Engineering, 1513
Sandia National Laboratories[2]
P.O. Box 5800
Albuquerque, NM USA 87185

J. Holen and B. F. Magnussen
Division Thermodynamics
SINTEF/Norwegian Inst. Tech.
Trondheim, Norway N-7034

Submitted for presentation at the Fourth International Symposium on Fire Safety Science, Ottawa, Canada, June 13-17, 1994

Abstract

A comparison of the KAMELEON Fire model to large-scale open pool fire experimental data is presented. The model was used to calculate large-scale JP-4 pool fires with and without wind, and with and without large objects in the fire. The effect of wind and large objects on the fire environment is clearly seen.

For the pool fire calculations without any object in the fire, excellent agreement is seen in the location of the oxygen-starved region near the pool center. Calculated flame temperatures are about 200 - 300 K higher than measured. This results in higher heat fluxes back to the fuel pool and higher fuel evaporation rates (by a factor of 2). Fuel concentrations at lower elevations and peak soot concentrations are in good agreement with data.

For pool fire calculations with objects, similar trends in the fire environment are observed. Excellent agreement is seen in the distribution of the heat flux around a cylindrical calorimeter in a rectangular pool with wind effects. The magnitude of the calculated heat flux to the object is high by a factor of 2 relative to the test data, due to the higher temperatures calculated. For the case of a large flat plate adjacent to a circular pool, excellent qualitative agreement is seen in the predicted and measured flame shapes as a function of wind.

Introduction

The mathematical modeling of fires and their effects on structures is an important aspect of fire safety science. If a fire and its consequences can be modeled mathematically, then the model can be used

1. Author to whom correspondence should be addressed.

2. Sandia National Laboratories is operated for the U. S. Department of Energy under contract #DE-AC04-76DP00789.

to predict fire environments and their impact, as well as to explore possible mitigation and fire-hardening strategies. The result of the development and application of such a model will be an increased level of fire safety.

Large-scale, open pool fires represent an important class of fire safety problems. A few examples include fires resulting from aircraft crashes, accidents involving hazardous waste shipping containers, and petroleum drilling platform accidents. There are very few fire models that are capable of calculating large-scale open pool fire environments from a 'first principles' basis (i.e., from the basic governing equations and without a high dependence upon experimentally developed correlations). For the models that do exist, there has been only limited comparison to large-scale open pool fire experimental data (see for example, [1-2]). Therefore, validation of these models against large-scale open pool fire data remains an important objective.

KAMELEON Fire is a state-of-the-art fire field model for the calculation of fire environments and their impact on structures. While KAMELEON Fire was specifically developed for application to fires in the petroleum drilling industry, it can be used to model many fire environments of common interest, such as jet fires, pool fires, and enclosure fires. This paper discusses a comparison of calculations performed with the KAMELEON Fire model to large-scale open pool fire experimental data.

Numerical Model

KAMELEON Fire has been developed over the last 20 years at the SINTEF Foundation and the Norwegian Institute of Technology (NTH), and has been primarily applied to model fires in offshore petroleum drilling platforms (see Holen, et al. [1]). The numerical methods in KAMELEON Fire are based on the work done by Hjertager [3], and Berge [4] who developed a general purpose heat and mass transfer model known as KAMELEON. Since only a brief summary of the model will be given in this paper, the interested reader should refer to the above references for more details.

KAMELEON Fire uses an extension of the SIMPLE method of Patankar and Spalding [5] to solve the conservation equations for mass, momentum, and energy transport on a finite difference grid. First-order upwind differencing is used for the convective terms in the discretized partial differential equations. A staggered grid is employed to solve for the velocities in 3 dimensions. The k-ε model of Launder and Spalding [6] is used to model the turbulence in the flow. The k-ε turbulence model was selected because of its wide use in engineering problems. Thus its strong and weak points are relatively well known.

The combustion model in KAMELEON Fire is based on Magnussen's Eddy Dissipation Concept (Magnussen and Hjertager [7], Magnussen et. al. [8]). The Eddy Dissipation Concept (EDC) is a general concept for describing the interaction between the turbulence and the chemistry in flames. The EDC assumes that the combustion process occurs in the turbulent fine structures, which are modeled as perfectly stirred reactors. Presently, KAMELEON Fire uses irreversible combustion assumptions in the combustion model. The EDC could also be formulated in terms of other assumptions (such as equilibrium chemistry or finite rate chemistry), if so desired. Presently, the combustion process in KAMELEON Fire is assumed to occur infinitely fast, i.e., it does not include finite rate chemistry. However, an extinction test is included in the model. Local extinction is assumed to occur when the time scale for turbulent mixing (calculated by the model) is less than the chemical time scale (input by the user).

The modeling of soot formation is based on a two-step process first proposed by Tesner, et al. [9] for acetylene fuel. The first step treats the formation of radical nuclei, and the second step the formation of soot particles from the radical nuclei. Magnussen [10] has modified the formulation for application to fuels other than acetylene. Once soot is formed, the EDC is capable of modeling the combustion of soot in the flame.

Thermal radiation of the combustion products (including soot) is modeled using the Discrete Transfer Method of Shah and Lockwood (see Shah, [11]). This method is used primarily because it represents an acceptable compromise between computational speed and accuracy for many problems. The soot and combustion gases are treated as a gray gas with an effective absorption and emission coefficient.

The eddy viscosity near solid surfaces is calculated using the logarithmic wall function method of Launder and Spalding [6]. No convective heat transfer is modeled to objects in the flow field.

KAMELEON Fire is capable of modeling fires that are enclosed as well as fires that are out in the open. Thus, both pool fires and jet fires can be modeled. Constant velocity wind boundary conditions can be specified.

Extensive pre- and post-processing tools have been developed for use with the general heat and mass transfer model, KAMELEON. These pre- and post-processors are also very useful for generating a grid and input deck for KAMELEON Fire, as well as interpreting the KAMELEON Fire results.

KAMELEON Fire Results

Pool fire calculations were conducted with KAMELEON Fire for pool fires with and without objects in them. Pool fires *without* objects in them are of interest to determine how well the model can predict the fire environment. Pool fires *with* objects in them are of interest to determine how well the model predicts the effect of the environment on an object.

Circular Pool Fire without Objects

The test data used for comparison for the circular pool without objects was supplied by Mansfield [12], and is for a 15 m diameter pool of JP-4 jet fuel, approximately 35 mm in depth. Accompanying details are taken from Raj [13]. For these tests, there was virtually zero wind conditions. These tests were selected for comparison because of the size of the pool and the amount of instrumentation present within the flame volume.

Calculations were carried out for an ambient pressure of 1 bar, ambient temperature of 290 K, zero wind conditions, pool level with the ground (thickness of 35 mm), chemical time scale of $5.x10^{-5}$ s, freestream turbulent length scale of 2 m, freestream turbulence intensity of 0.2, turbulent length scale just above the pool of 2 m, and a turbulence intensity right above the pool of 0.0164. A 30 x 20 x 35 non-uniform grid was used to model a 50 m x 25 m x 70 m volume, with a symmetry plane through the center of the pool normal to the shortest (25 m) axis.

A plot of the local temperature field is shown in Figure 1 for a vertical plane close to the center of the fuel pool. All of the figures shown for this case are for a time of 3 minutes following ignition. Calculations were carried out longer (for about 5 minutes) with little difference in the results. The calculated flame height is 57 m (arbitrarily taken to be the maximum height of the 1100 K isotherm). This is 27% higher than the visual estimate of a 45 m flame height for the test.

Figure 2 shows a more detailed temperature plot for the same plane in the fire. The experimentally measured temperatures are shown in Figure 3 for comparison. Calculated flame temperatures are approximately 200-300 K higher than the measurements indicate. It is noted that the model does an excellent job of predicting the size and shape of the oxygen-starved region in the center of this large pool fire, and the sharp gradients in temperature near the edge of the flame where oxygen is readily available. The size and shape of the first 6 meters of flame elevation are also very well predicted by the model. However, at elevations greater than 6 m the calculated shape differs from the measured temperature profile. If the measured temperature profile is assumed to be representative of the flame diameter, the measured flame volume expands slightly between 6 and 14 m, and then begins to decrease very gradually beyond about 14 m. The calculations do not indicate this region of slight expansion, but do show the very gradual decrease in flame radius with elevation.

There are several possible reasons for the calculated flame temperatures being larger than the measured temperatures. This could be due to radiative, convective, and/or soot effects regarding the thermocouple measurements. It could also be due to the irreversible combustion model in KAMELEON Fire. KAMELEON Fire assumes that all of the fuel and oxidizer that are mixed into the turbulent fine structures react to form products (assuming the time scale for turbulent mixing is long enough). In view of this assumption, and also the fact that no dissociation reactions are modeled, more fuel can be combusted and calculated flame temperatures can be higher than actually present in a flame. Incorporation of an equilibrium chemistry model with dissociation effects into KAMELEON Fire is planned in the near future.

It is interesting to compare the fuel evaporation rate from the pool. The calculated fuel evaporation rate of approximately 0.16 $kg/m^2/s$ (averaged over the pool) is two times as large as the measured value. This is consistent with previous comparisons between KAMELEON Fire pool fire results and experiments (Oppstad, et al.[14]). If, in fact, the flame temperatures calculated with KAMELEON Fire are too high (as discussed above), this would lead to higher radiative heat fluxes back to the fuel pool and result in higher fuel evaporation rates. A quick estimate indicates that the radiative heat flux back to the fuel pool, which goes as the fourth power of the absolute gas temperature, would be roughly a factor of $(1700\ K/1400\ K)^4 = 2.17$ too high. Therefore, this discrepancy between the calculated and measured fuel evaporation rates is highly consistent with the discrepancy in flame temperature.

A comparison of the unburned fuel mass fraction along the vertical centerline of the fire is shown in Table 1. It can be seen that the

TABLE 1 Fuel and Soot Concentrations at Pool Centerline (Data from [12])

Height Above Pool (m)	Measured Fuel Concentration (kg/kg)	Calculated Fuel Concentration (kg/kg)	Measured Soot Concentration (kg/kg)	Calculated Soot Concentration (kg/kg)
0.7	0.43 - 0.45	0.35 - 0.40	0.002	>0.08
1.4	0.40 - 0.46	0.30 - 0.35	0.0 - 0.007	>0.08
2.8	0.31 - 0.38	0.25 - 0.30	0.006 - 0.012	0.065 - 0.07
5.7	0.17 - 0.22	0.20 - 0.25	0.015 - 0.023	0.05 - 0.055
11.4	0.03 - 0.05	0.15 - 0.20	0.025 - 0.034	0.028 - 0.033
22.8	0.02	0.05 - 0.10	0.015	0.011

calculated values are in good agreement with the measured values (which are slightly larger) at elevations below 11.4 m. This is somewhat surprising in view of the difference in calculated and measured pool evaporation rates. Above 11.4 m, the KAMELEON Fire calculations over-predict the measured fuel concentrations. It is possible that the irreversible combustion model in KAMELEON Fire may over-predict the burning of fuel at lower elevations in the flame, and thereby compensate for the over-prediction of the burning rate. It should also be remembered that the collection and interpretation of experimental data in large fires is difficult, and is not without its own uncertainty.

The calculated maximum soot mass fraction varied between 0.01 and 0.1, fluctuating from time step to time step. This range agrees well with the measured values of 0.025-0.034. However, comparison to the experimental results (along the vertical centerline of the fire) indicates that the trends are different between the two (Table 1). The calculated results indicate a gradual decrease in soot mass fraction with elevation (apart from the first meter just above the fuel surface). The values measured by Mansfield show a gradual increase in soot concentration to a maximum value at an elevation of 11.4 m, and then a gradual decrease. However, recent absorption coefficient measurements by one of the authors (Gritzo, [15]) indicate that the soot concentration may in fact be a steadily decreasing function of elevation, as predicted by the model.

Rectangular Pool with Cylindrical Calorimeter

Pool fire calculations were also conducted with KAMELEON Fire for pool fires with objects in them. The test data used for comparison was taken from Schneider, et al [16] for a 9 m x 18 m pool of JP-4 jet fuel. For these tests, the winds were out of the southwest (on average), with components of 4.46 m/s from the west, and 2.47 m/s from the south. A large cylindrical calorimeter of diameter equal to 1.4 m, and length equal to 7 m was placed in the fire, with its base roughly 1 m above the fuel surface (see Figure 4, which is a view of the pool from above).

Calculations were carried out for an ambient pressure of 1 bar, ambient temperature of 290 K, constant wind conditions as specified above, pool level with the ground, chemical time scale of $5.x10^{-5}$ s, freestream turbulent length scale of 2 m, freestream turbulence intensity of 0.2, turbulent length scale just above the pool of 2 m, and a turbulence intensity right above the pool of 0.0164. A constant fuel evaporation rate of 0.077 $kg/m^2/s$ was specified, since the calculations with the circular pool indicated that the burning rate would be over-predicted by KAMELEON Fire. A 20 x 30 x 30 non-uniform grid was used to model a 30 m x 60 m x 70 m volume, without any symmetry planes.

The following results correspond to a time of 6 minutes following the ignition of the fire. Figure 5 shows a projection of the calculated flame shape (with the calorimeter superimposed upon it). The calculations indicate that much of the calorimeter is actually engulfed by the flames, but it will be shown in the figures as superimposed upon the fire. The effect of the wind is clearly seen in Figure 5, as the fire leans to the north side (the view in Figure 5 is from the west side of the pool). Figure 6 shows a view of the fire from the south side. The wind effect is again clearly seen, this time causing the flame to develop a greater size along the east side of the pool, and further downwind.

A longitudinal slice through the calorimeter indicates that only a portion of the top surface of the calorimeter is engulfed by flames (the center portion of the calorimeter), as seen in Figure 7. The top of the calorimeter is exposed (no flame coverage) along the north and south ends (the view in Figure 7 is from the west side). The velocity vectors shown in this figure clearly show the effects of the cross-wind. A large recirculation region is located near the north end of the object.

The temperatures show reasonable agreement with the experimental measurements, with calculated temperatures approximately 200 - 300 K higher than measured. The calculated heat flux to the north end of the calorimeter can also be compared to data. As shown in Table 2, the

TABLE 2 Measured vs. Calculated Heat Flux to Calorimeter

Location	**Measured Heat Flux (kW/M^2)**	**Calculated Heat Flux (kW/M^2)**
Top	25	39
Bottom	150	333
East	90	144
West	60	119

calculated heat flux is roughly two times higher than measured (again due to the larger temperatures). Excellent agreement is observed in the distribution of the heat flux around the circumference of the calorimeter. Figure 8 is useful in interpreting the heat flux distribution, and again demonstrates the non-uniformity in flame coverage around the calorimeter. This figure shows a vertical slice through the north end of the calorimeter, as seen from the south side of the pool. Velocity vectors are used to describe the flow field.

The flame coverage along the surface of the calorimeter appeared to be changing slowly with time. The above comparison represents a snapshot in time, and the results may be different later in time. Also, KAMELEON Fire presently only allows for constant temperature objects. Transient heat up of an object is not modeled. The north end of the calorimeter was very thermally massive, and as such, could be assumed to remain near the initial temperature during the early part of the test (thus allowing the above heat flux comparison to be made).

Circular Pool Fire with Flat Plate

A further comparison of KAMELEON Fire results with large-scale pool fire data can be made based on recent tests conducted at the Naval Air Warfare Center (NAWC) at China Lake, California. A series of 3 tests was performed. For all tests, a thermally massive flat plate calorimeter (2.1 m wide x 5.2 m high) was placed on the edge of a 19 m diameter pool of JP-4 fuel (tangent to the pool circumference). The object of these tests was to investigate the interaction between a large, thermally massive object and the fire environment (Nicolette and Larson [17], Gritzo and Nicolette [18]).

Because of the recent time-frame of these tests, only qualitative comparisons can be made at the present time (the experimental data has not yet been reduced). Therefore, a brief discussion of the qualitative results of the tests is necessary for comparison to the calculations. The first test was initiated under no-wind conditions (<0.22 m/s). Following ignition, a continuous flame developed which became fully attached to the surface of the plate (i.e., the entire flame volume was attached to the plate, and the plate was fully engulfed by flame). A constant wind speed of 0.89 m/s in a direction normal to the front surface of the plate was measured at an elevation of 5 m and a radial distance of 10 m from the pool boundary. Based on the observed flame shape, it was concluded that the plate provided a sufficient restriction to the air entrainment process for the entire flame to be drawn to the plate. The 0.89 m/s wind speed measured was assumed to be fire-induced.

This first test was modeled with KAMELEON Fire by imposing a zero wind velocity boundary condition in the far-field (at a distance of 25 m from the pool boundary). The model predicted a quite different flame behavior than observed in the first test. Calculations showed a primary flame region which necked sharply near the ground level, and then rose vertically upward normal to the ground (i.e., the main flame was NOT pulled over and attached to the plate). A second flame zone was predicted by the model to intermittently attach along the plate surface. This can be seen in Figure 9. Note the gap between the main flame volume and the small flame region attached to the plate surface. Because these results disagreed with the observed flame shape of the first test, a second calculation was performed with a wind boundary condition of 0.89 m/s imposed at the far-field boundary. For this calculation, the model predicted that the flame laid over at a sufficient angle to engulf the plate (in excellent agreement with the results of the first test). Thus, KAMELEON Fire was indicating that the measured wind speed of 0.89 m/s in the first test was not entirely fire-induced, but resulted from an actual wind.

Following these calculations, a second test was performed under no-wind conditions (in a manner consistent with the first test). For this test, measured wind speeds (monitored at the same location as in the first test) remained constant following ignition at < 0.44 m/s (significantly lower than in the first test). In this test, the flame volume rose vertically with extensive necking near the pool surface as seen in Figure 10. A strong secondary flame zone was observed to be attached to the plate and is denoted with an arrow in Figure 10. Note the gap between the flame attached to the plate and the main flame volume, and compare to Figure 9. The secondary flame zone attached to the plate is produced by the restriction of air flow into the main flame as a result of the blockage effect of the plate. This obstruction results in a highly-mixed region on the front surface of the plate which produces the secondary flame zone.

These results indicate excellent qualitative agreement between KAMELEON Fire calculations and experimentally observed flame shapes. This comparison is especially significant since the model predictions were obtained before the second test was conducted.

Summary

KAMELEON Fire has been used to model large-scale open pool fires with and without objects, and with and without winds present. The model showed generally good agreement with test data.

For the pool fire calculations without any object in the fire, excellent agreement is seen in the location of the oxygen-starved region near the pool center. Calculated flame temperatures are about 200 - 300 K higher than measured. This results in higher heat fluxes back to the fuel pool and higher fuel evaporation rates (by a factor of 2). Fuel concentrations at lower elevations and peak soot concentrations are in good agreement with data, although the soot distribution throughout the flame may be subject to question.

For pool fire calculations with objects, similar trends in the fire environment are observed. The effect of an external wind can be clearly seen in the calculated results. Excellent agreement is seen in the distribution of the heat flux around a cylindrical calorimeter. The magnitude of the calculated heat flux to the object is high by a factor of 2 relative to the test data, due to the higher temperatures calculated. For the case of a large flat plate adjacent to a circular pool, excellent qualitative agreement is seen in the predicted and measured flame shapes as a function of wind. The prediction of a secondary flame zone attached to the plate is confirmed by experiment.

References

1. Holen, J., Brostrom, M., and Magnussen, B. F., Finite Difference Calculation of Pool Fires, The 23rd Symposium (International) on Combustion, pp. 1677-1683, 1990.

2. Harsha, P. T., Bragg, W. N., Edelman, R. B., Mathematical Model of a Large Open Fire, Science Applications Incorporated, Canoga Park, CA, report # SAI-81-026-CP, April 1981.

3. Hjertager, B. H., Flow, Heat Transfer and Combustion in Three-Dimensional Rectangular Enclosures, Dr. ing. thesis, University of Trondheim, Norwegian Institute of Technology, Division of Thermodynamics, 1979.

4. Berge, G., Numerisk programsystem basert pa fleirdimensjonale ortoganale koordinatar for simulering av forbrenning, masse- og varme-transport, Dr. ing. thesis, University of Trondheim, Norwegian Institute of Technology, Division of Thermodynamics, 1987.

5. Patankar, S. V., and Spalding, D. B., International Journal of Heat and Mass Transfer, vol. 15, p. 1787, 1972.

Review Copy

6. Launder, B. E., and Spalding, D. B., Computer Methods in Applied Mechanics and Engineering 3, p. 269, 1972.

7. Magnussen, B. F., and Hjertager, B. H., The Sixteenth Symposium (International) on Combustion, The Combustion Institute, 1976.

8. Magnussen, B. F., Hjertager, B. H., Olsen, J. G., and Bhaduri, D., The Seventeenth Symposium (International) on Combustion, The Combustion Institute, p.1383, 1979.

9. Tesner, P. A., Snegiriova, T. D., and Knorre, V. G., Combustion and Flame, vol. 17, p. 253, 1971.

10. Magnussen, B. F., "The Eddy Dissipation Concept," Proceedings of the Eleventh Task Leaders Meeting, IEA Working Party on Conservation in Combustion, Lund, Sweden, 1989.

11. Shah, N. G., The Computation of Radiation Heat Transfer, Ph.D. thesis, University of London, Faculty of Engineering, 1979.

12. Mansfield, J. A., JM Technical, personal communication, January 1993.

13. Raj, P. K., Analysis of JP-4 Fire Test Data and Development of a Simple Fire Model, ASME paper no. 81-HT-17, 1981.

14. Oppstad, K., Wighus, R., Holen, J., Hekkelstrand, B., and Stensaas, J. P., Modeling of Hydrocarbon Fires Offshore, SINTEF Foundation, SINTEF report no. STF25 A91029, 1991.

15. Gritzo, L. A., Sandia National Laboratories, unpublished data, September 1993.

16. Schneider, M. E., Keltner, N. R., and Kent, L. A., Thermal Measurements in the Nuclear Winter Fire Test, Sandia National Laboratories, SAND88-2839, January 1989.

17. Nicolette, V. F., and Larson, D. W., "The Influence of Large Cold Objects on Engulfing Fire Environemnts," Heat and Mass Transfer in Fires, ASME HTD Vol. 141, 1990.

18. Gritzo, L. A., and Nicolette, V. F., "Coupled Thermal Response of Objects and Participating Media in Fires and Large Combustion Systems," Heat Transfer in Fires and Combustion Systems, ASME HTD Vol. 250, pp. 161-172, 1993.

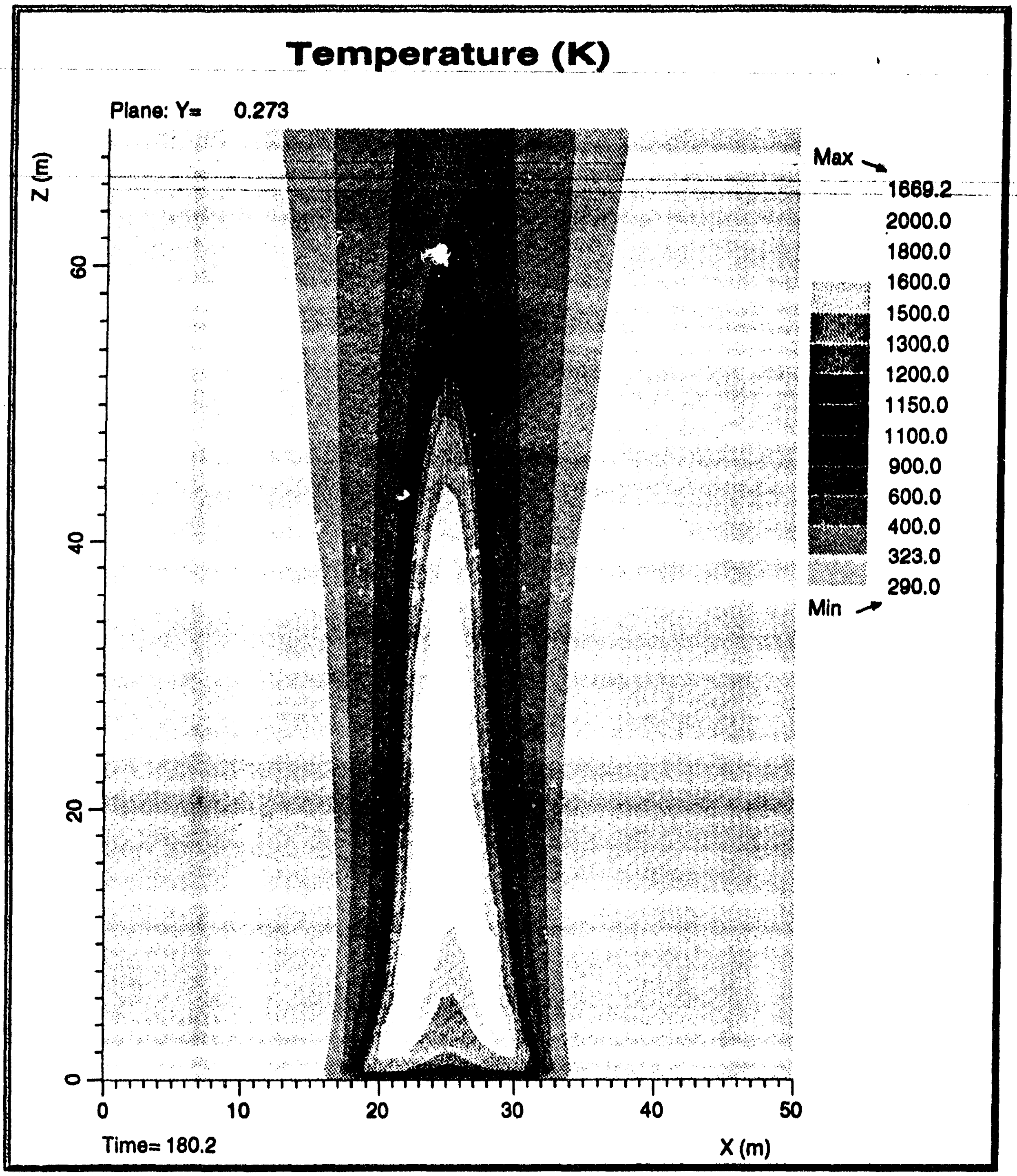

Figure 1. Circular Pool Fire (15 m Diameter): Calculated Flame Shape

Note: Original Figure is in Color. Can be converted to gray scales if desired.

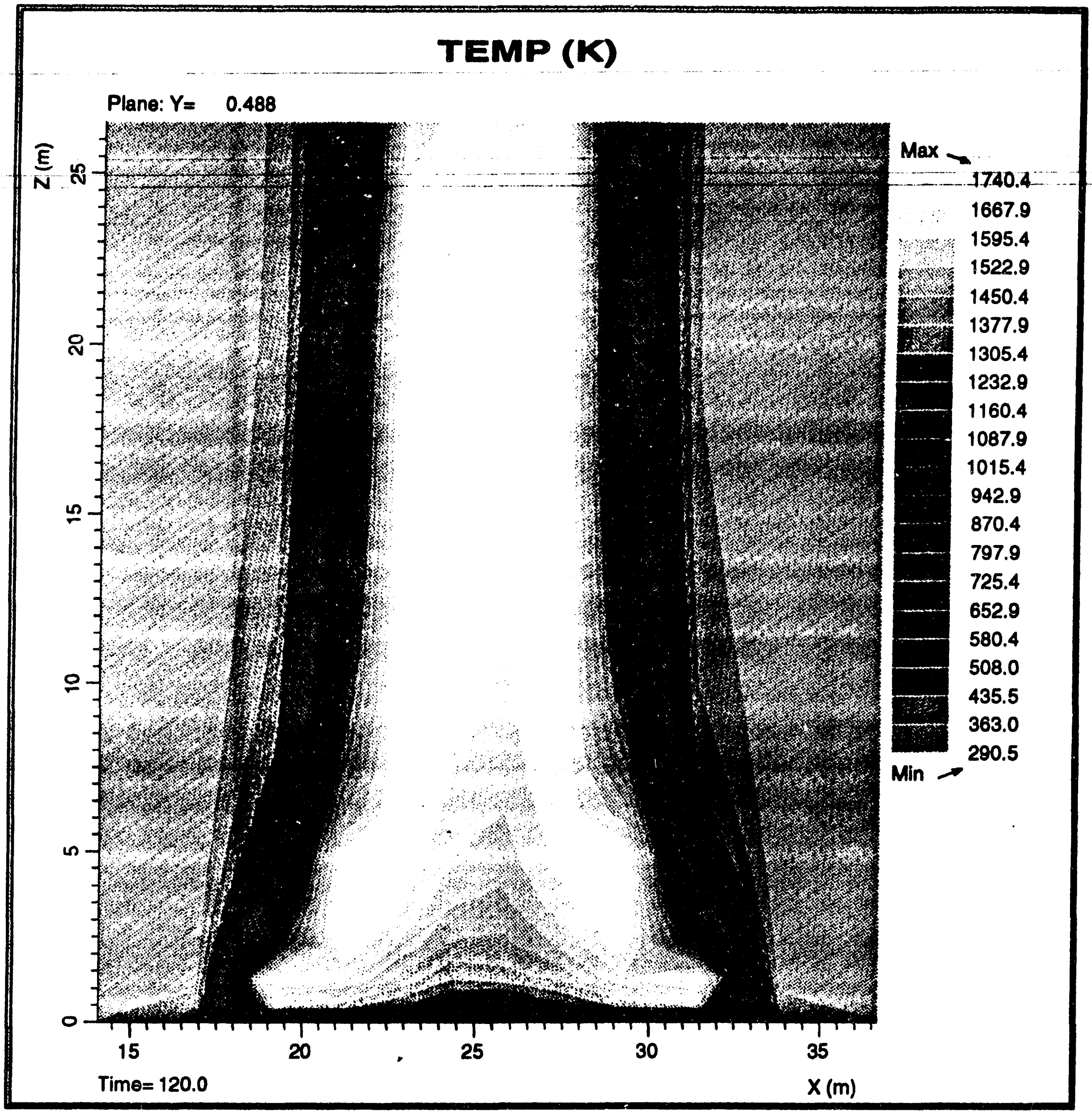

Figure 2. Circular Pool Fire (15 m Diameter): Calculated Isotherms

Note: Original Figure is in Color. Can be converted to gray scales if desired.

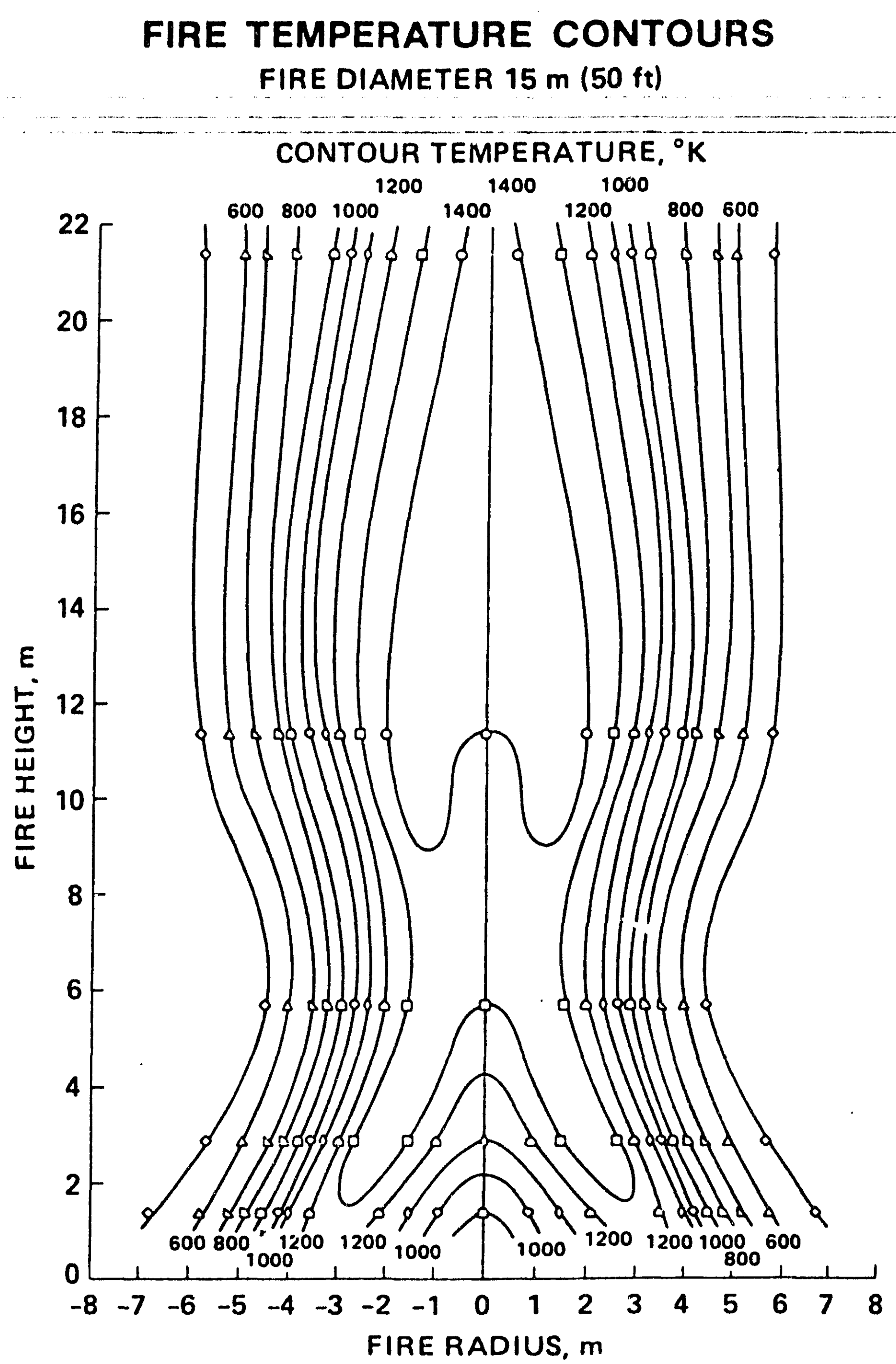

Figure 3. Experimentally Measured Pool Fire Isotherms (15 m Diameter) [12]

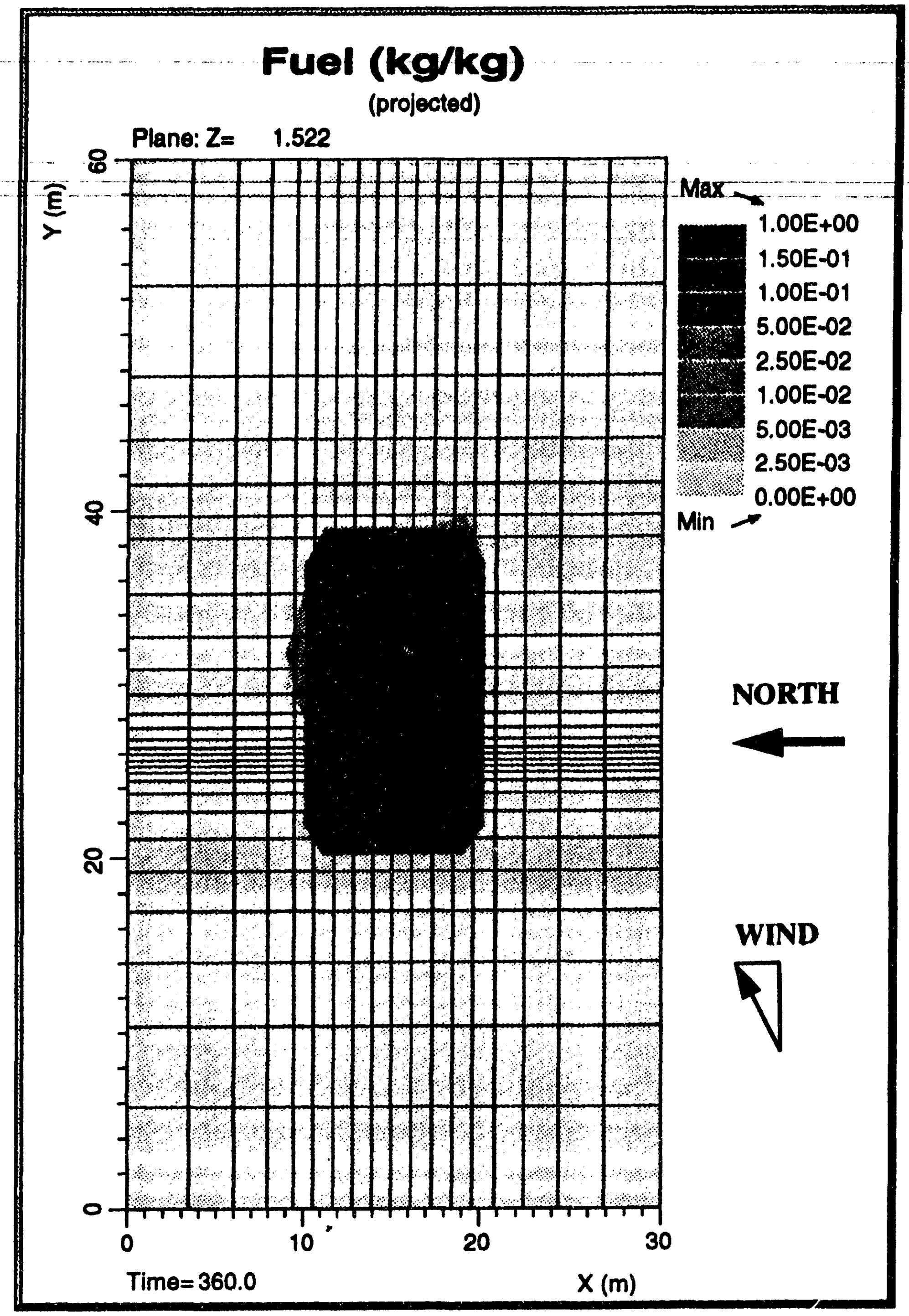

Figure 4. Rectangular Fuel Pool (9m x 18m) with Object and Wind
(View is from Above)

Note: Original Figure is in Color. Can be converted to gray scales if desired.

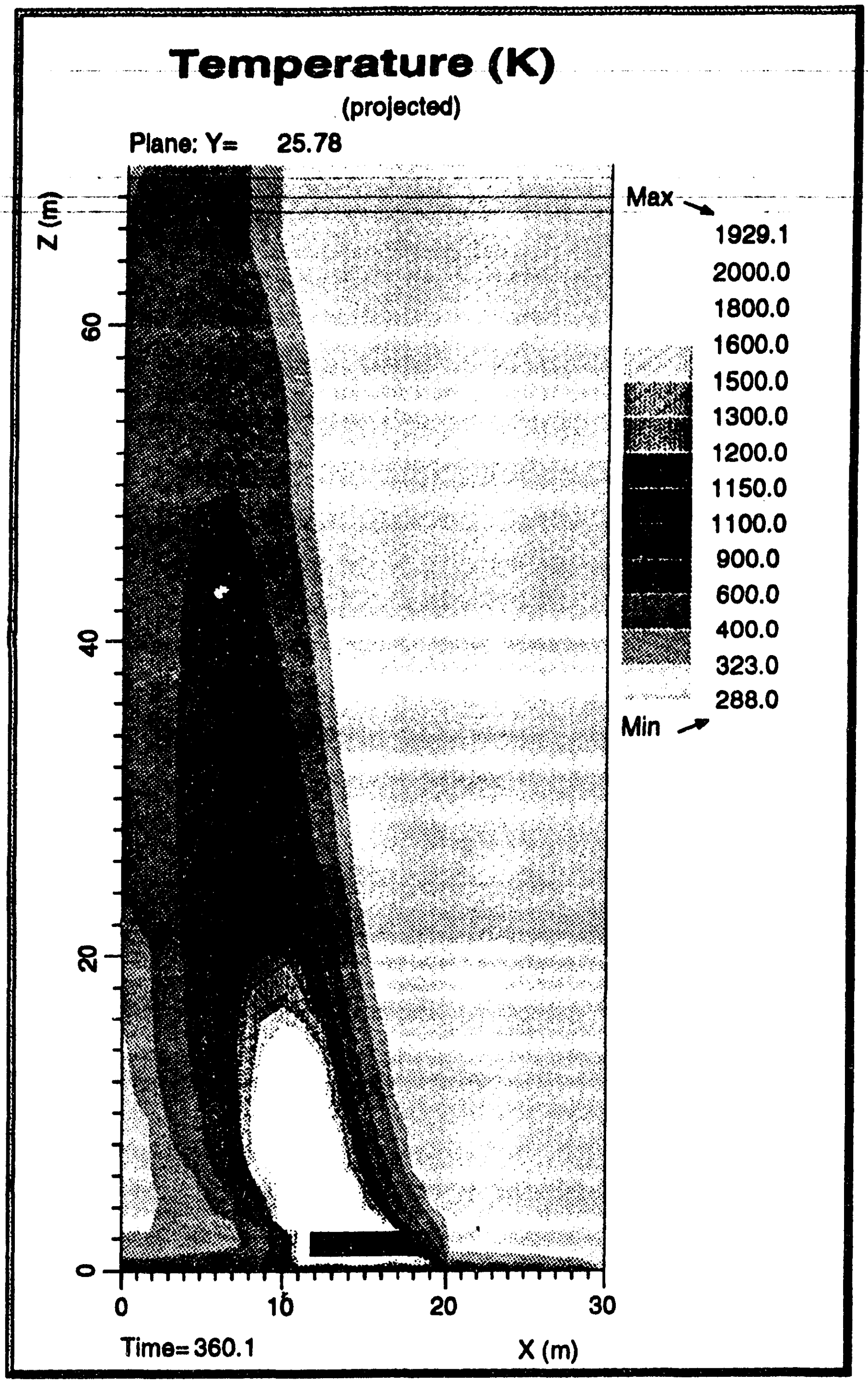

Figure 5. Rectangular Pool Fire Flame Shape with Wind and Object (View is from West Side of Pool)

Note: Original Figure is in Color. Can be converted to gray scales if desired.

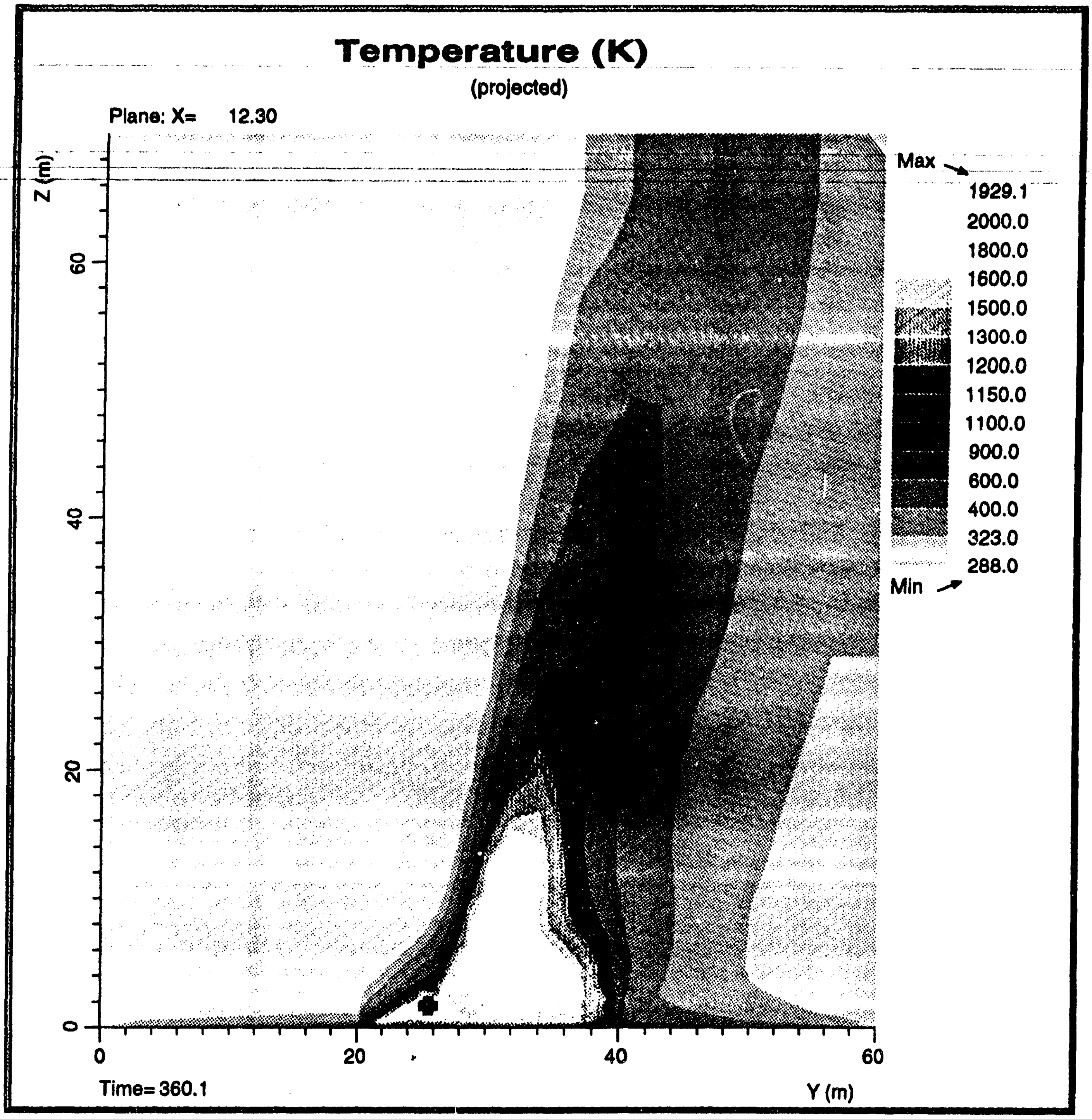

Figure 6. Rectangular Pool Fire Flame Shape with Wind and Object
(View is from South Side of Pool)

Note: Original Figure is in Color. Can be converted to gray scales if desired.

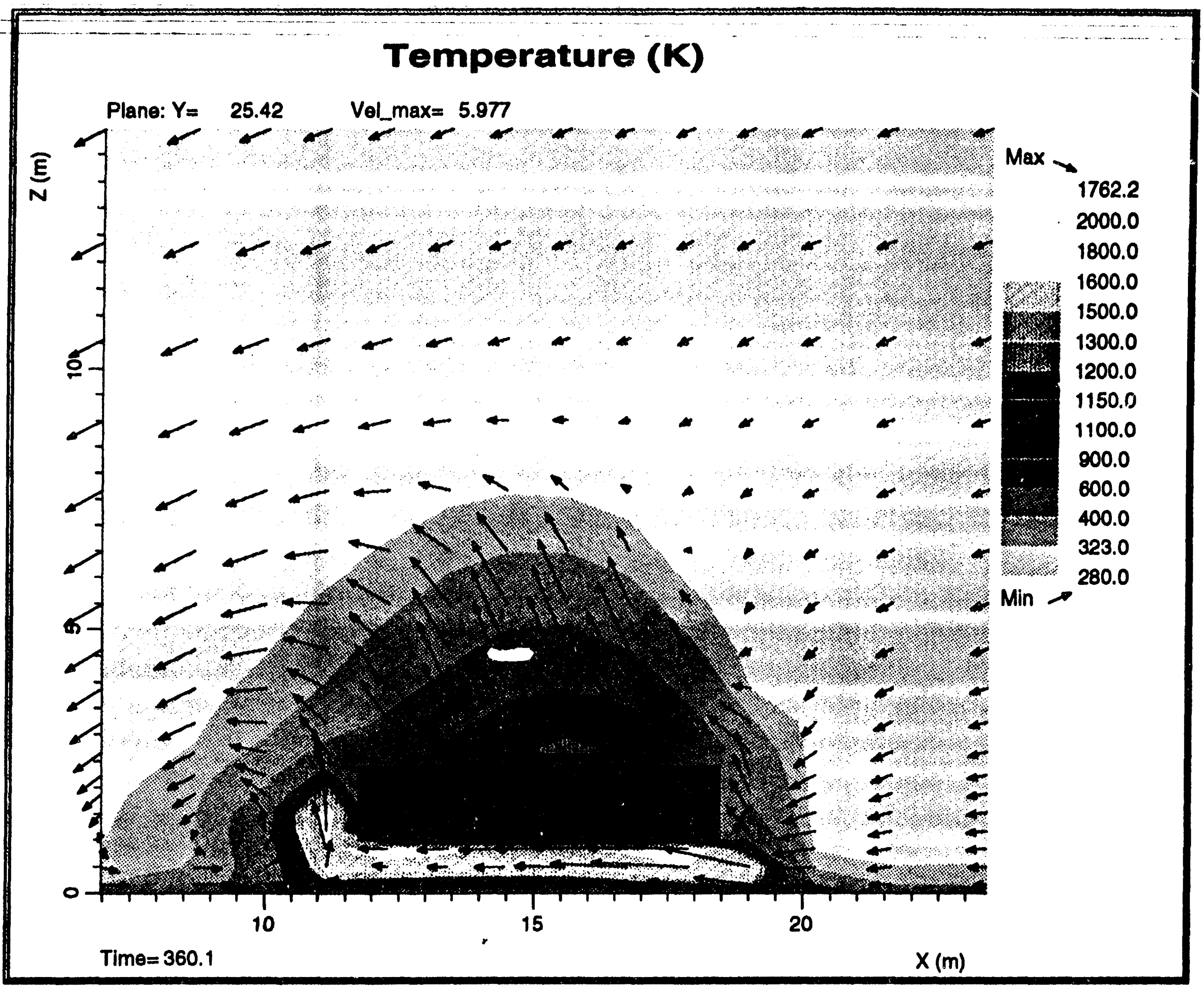

Figure 7. Rectangular Pool Fire with Wind and Object: Vertical Slice Through Object (View from West Side) Showing Isotherms and Velocity Vectors

Note: Original Figure is in Color. Can be converted to gray scales if desired.

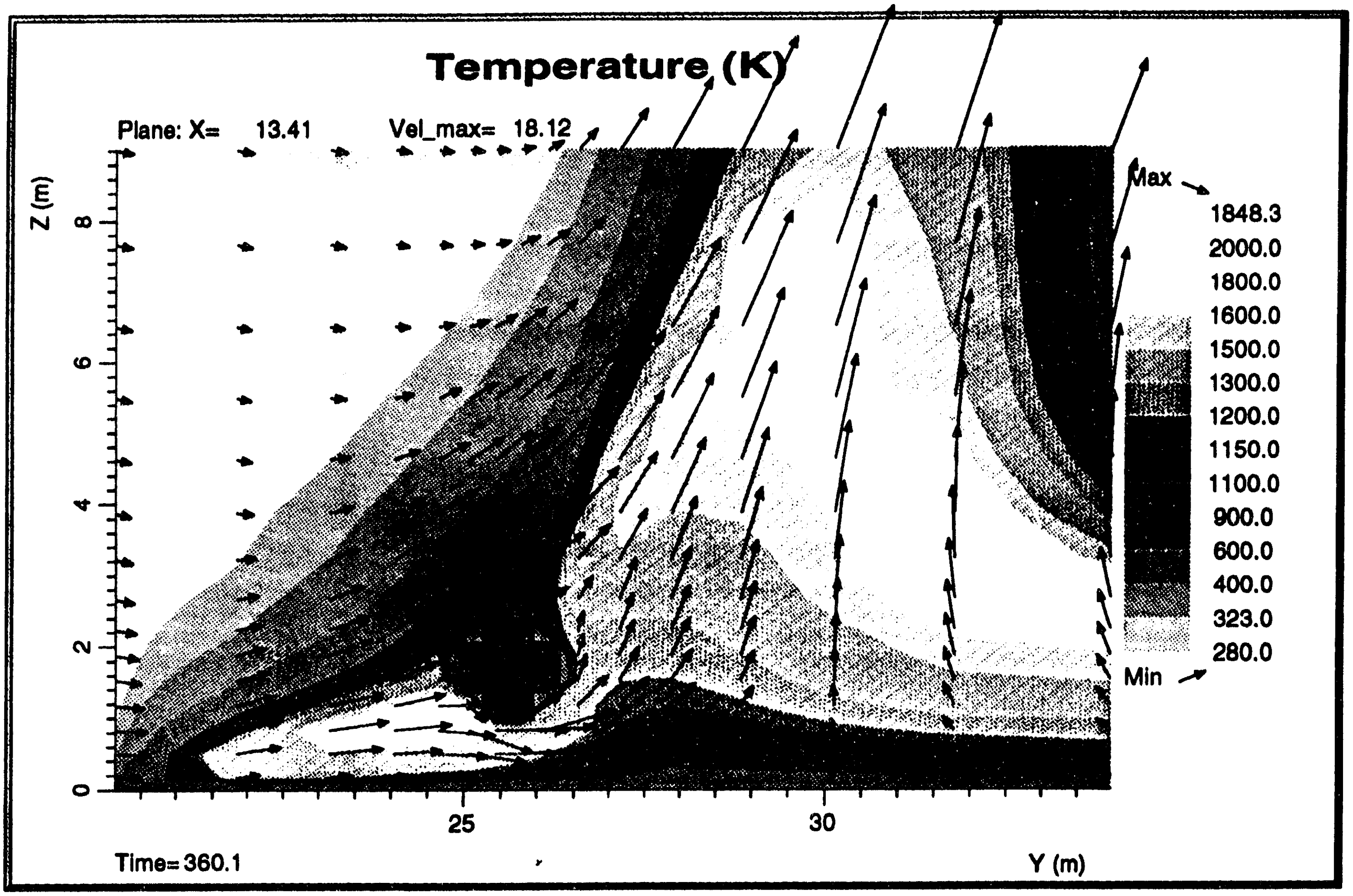

Figure 8. Rectangular Pool Fire with Wind and Object: Isotherms and Velocity Vectors near North End of Object (View from South Side)

Note: Original Figure is in Color. Can be converted to gray scales if desired.

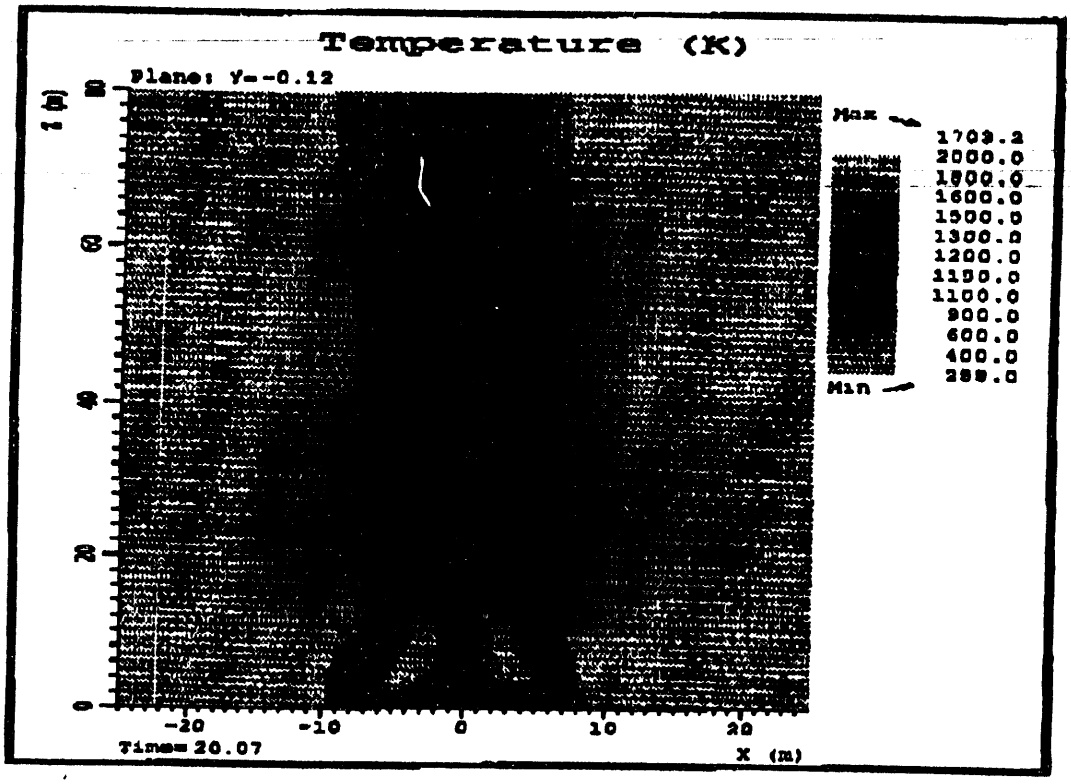

Figure 9. Circular Pool (19 m Diameter) with Plate: Isotherms Showing Calculated Flame Shape (Note Secondary Flame Attached to Plate)

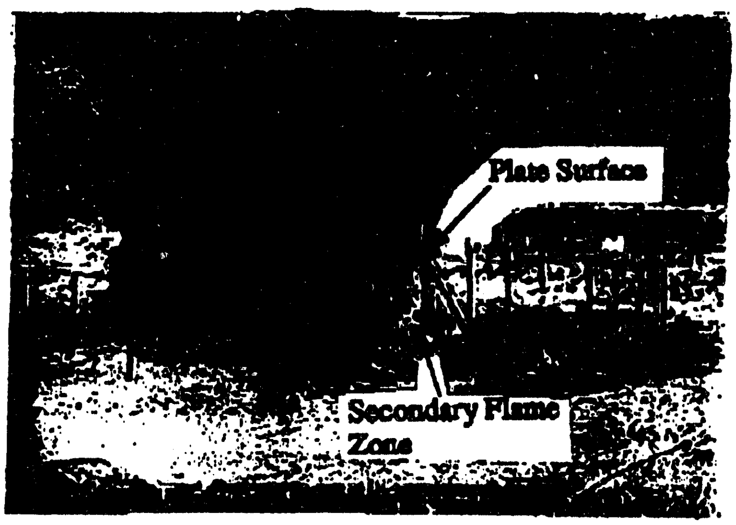

Figure 10. Circular Pool (19 m Diameter) with Plate: Photograph of Experimentally Observed Flame Shape (Note Secondary Flame Attached to Plate)

Note: Original Figure and Photograph are in Color, and are high quality. They have reproduced very poorly for this review copy.

DATE
FILMED
8/2/94

END